SHERPA: A Spectrometer with High Energy Resolution and Polarisation Analysis

Kirill Nemkovski[1], *Robert* Bewley[1], *Victoria* García Sakai[1], *Gøran Jan* Nilsen[1], *Adrien* Perrichon[1], and *Ian* Silverwood[1*]

[1]ISIS Neutron and Muon Source, STFC Rutherford Appleton Laboratory, Harwell Science and Innovation Campus, Didcot, Oxfordshire, OX11 0QX, UK

Abstract. SHERPA is a proposed quasielastic neutron spectrometer with polarisation analysis, intended to replace the ageing Iris instrument at the ISIS neutron and muon source. In this paper we present a concept of the instrument along with Monte-Carlo simulations and analysis of possible instrument location. We expect greatly increased count rate compared to Iris (expected from 49 to 660 × Iris) in unpolarised mode and dedicated polarisation analysis capabilities at a more modest count rate increase (~5-70 × Iris). This huge gain in the count rate would be achieved from the combination of three factors: modern neutron guide with high-m coating, and prismatic effect and larger solid angle coverage at the energy analyser. Such an instrument would be the first of its kind and has incredible potential to revolutionise quasielastic neutron scattering technique through the separation of the coherent and incoherent scattering contributions.

1 Introduction

Quasielastic neutron scattering (QENS) is widely used to study dynamics at the atomic and nanoscale in a wide variety of systems including confined materials, [1,2] proteins,[3] polymers,[4,5]ionic liquids [6,7] and solid electrolytes.[8,9] Depending on the scientific problem, it may be important to obtain the purely incoherent or coherent scattering components, which correspond to the individual or collective *and* individual motions of the atoms, respectively. However, since the unpolarised experiment measures the sum of these two contributions, one component can mask the other, thus complicating the analysis of the experimental data.

In many cases, this problem can be effectively solved using neutron polarisation analysis (PA) methods. Recent measurements on direct geometry time-of-flight (ToF) spectrometers such as LET at the ISIS Neutron and Muon Source, UK,[10,11] D7 at the Institute Laue-Langevin, France, [7,12] and the multi-axis crystal spectrometer MACS at the NIST Center for Neutron Research, USA [13] have demonstrated the benefits of PA for this.

On the other hand, many QENS experiments require access to a broad range of energy transfer and a relatively high energy resolution, in order to gain insight into dynamical processes that take place over several decades in time up to nanoseconds. Direct geometry spectrometers have a limit to the resolution they can achieve, with stricter incident monochromation unavoidably leading to lower flux at the sample. Similarly, on triple-axis spectrometers (TAS), a higher energy resolution corresponds to lower values of the incoming/final energies, giving a smaller volume of the resolution ellipsoid and reduced count rate. Counting on single-detector TAS-type instruments is also more time consuming due to the need to scan $\boldsymbol{Q}$-E space point-to-point. Multiple-analyser spectrometers improve the situation, but do not eliminate the issue completely. Polarisation analysis further cuts the count rate and requires more time for measuring different neutron spin orientations. Very high energy resolution combined with some of the advantages of polarized neutrons is offered by the neutron spin echo technique. However, spin echo is also a low count-rate technique.

In contrast, indirect geometry near-backscattering ToF instruments on spallation sources offer benefits in terms of resolution, simplicity, cost, and above all, count rate, but currently there is no such instrument equipped with the ability to exploit polarised neutron analysis.

At ISIS there are two dedicated QENS instruments, Iris [14] and Osiris [15]. In fact, in the period from 2000 to 2005 there was considerable effort to develop PA-QENS on Osiris. However, although polarised diffraction was realised, only proof of concept was obtained with the inelastic mode.[16] Two major upgrades are in progress for Osiris to improve the flux and resolution by replacing the supermirror guide [17,18] and installing a silicon analyser,[19] but neither involve polarisation. In contrast, the future of Iris is still under discussion and the implementation of polarisation analysis is one opportunity being considered.

In this paper we describe a near backscattering spectrometer with dedicated polarisation analysis capabilities as a possible replacement for Iris. It would provide a similar momentum and energy transfer, ($\boldsymbol{Q}$

* Corresponding author: ian.silverwood@stfc.ac.uk

and *E)*, but considerable gains in flux and uniaxial polarisation analysis. The name of the concept is SHERPA: Spectrometer with High Energy Resolution and Polarisation Analysis.

Topically, the main focus of SHERPA is QENS in biological, soft matter and functional materials research. To better understand the requirements for such an instrument from potential users, we organized a dedicated workshop in March 2022. Based on the feedback, we can summarize that the soft matter community is primarily interested in higher energy resolution (< 10 μeV) compared to Iris. Increasing the flux is highly welcome, although not as important as good energy resolution. In opposition, studies of functional materials require rather high flux to be able to work with small samples, while the resolution can stay only moderately high (> 10 μeV). Though not the main target group, interest in high-count rate QENS with PA has also been expressed from the magnetism community. In all cases, it is also important to foresee the provision of sample environment such as furnaces, cryostats, and goniometers to align oriented samples (single crystals, thin films etc.)

2 SHERPA predecessor — Iris

Iris is a near-backscattering indirect geometry ToF spectrometer viewing the hydrogen moderator on Target Station 1 (TS1) at the ISIS Neutron and Muon Facility. It has remained largely unchanged since it was built in 1988.[20] It has a 36 m long neutron guide, which is coated with natural Ni ($m = 1$), ending with a 2.5 m long focusing snout with $m = 2$ coating. The sample position is located 36.5 m away from the moderator. The secondary spectrometer consists of two analyser banks made from pyrolytic graphite (PG) and mica. The corresponding detector banks consist of non-position-sensitive scintillator detectors and cover the scattering angle range of 25-160° for graphite and 25-155° for the mica. The graphite analyser provides an energy resolution of 17.5 μeV with the (002) reflection and is the workhorse setting of the instrument. However, the (004) can be used to access momentum transfers up to 3 $Å^{-1}$ with an energy resolution of 55 μeV. Although mica enables access to higher energy resolution (of 4.5 μeV with 004 and 1 μeV with 002), they are rarely used owing to the much-reduced flux.

3 SHERPA primary spectrometer

The most obvious upgrade to Iris is the complete replacement of the neutron guide with a modern one featuring a high m-value supermirror coating. An initial design has been performed based on recent developments for the "sibling" Osiris instrument.[17,18] Optimization was done via Monte Carlo simulations using the McStas ray-tracing package,[21-23] automated with an in-house MATLAB code. Amongst several guide geometries assessed, a curved guide with elliptical defocusing and focusing sections (see Fig. 1) was found to perform the best. The expected gain in flux is around a factor of 10. Note that

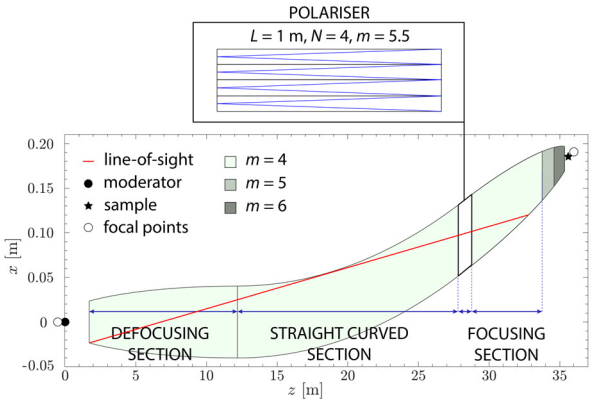

Fig. 1. SHERPA neutron guide with polarising section (see below). Reproduced and adapted from [18]. Model for instrument location on the Iris port.

the guide also includes the polarising section that will be discussed below.

4 SHERPA secondary spectrometer

As the most used configuration of Iris, we plan to use the (002) reflection from a pyrolytic graphite analyser with a Be filter to suppress higher orders of Bragg scattering.

The detector count rate is proportional to the incoming neutron flux Φ, the solid angle coverage of the analyser $d\Omega$ and wavelength acceptance of the analyser $\Delta\lambda$:

$$I \propto \Phi \cdot d\Omega \cdot \Delta\lambda \quad (1)$$

The wavelength acceptance of the analyser in turn depends on the crystal mosaicity μ, the analyser Bragg wavelength condition λ and cotθ :

$$\Delta\lambda = \mu \cdot \lambda \cdot \cot\theta \quad (2),$$

where θ is a half of the scattering angle on the analyser.

In backscattering geometry, θ is close to 90° in order to keep $cot\theta$ very small. To achieve the highest energy resolution. μ should be very small as well. On Iris, $\theta = 87.5°$ with $cot\theta = 0.04$, and $\mu = 0.8°$ (see Table 1). However, relaxing the constraint on either of these values would allow for significant gains in intensity. In a conventional backscattering instrument this gain would come alongside a loss in energy resolution. To resolve this, we propose here to use the prismatic effect proposed in the FARO concept,[24] which is already being explored for the future MUSHROOM [25] spectrometer at ISIS. Our initial simulations show that relaxing θ to 75.5° ($cot\theta = 0.26$), increasing the PG analysers solid angle by a factor of 3, and changing the mosaicity to 1.5° will achieve a factor 33 gain in intensity. This multiplied by the factor of 10 arising from the guide upgrade, would yield a game-changing total count rate gain of 330, or 660 if PG analysers are placed on both sides of the instrument. We will now demonstrate how this is achieved while simultaneously improving resolution.

The FARO concept is illustrated in Fig. 2(a). It uses the well-known Rowland circle where the sample, analyser and detector all touch the radius of a circle. This focuses neutrons from a point-like sample to a point on the detector with the same final energy while also keeping the final distance travelled almost constant

(important for resolution). The large mosaic spread of PG analyser crystals acts just like a prism to light, spatially separating the spread in analysed final energies (or wavelengths), so that as one moves up the position sensitive detector from the bottom the neutron energy is continually changing from higher energy to lower.

Table 1. Comparison (unpolarised) of two SHERPA options (see text) with IRIS and LET. Values for ΔE are given assuming a sample height of 10 mm.

	SHERPA TS1	SHERPA TS2	IRIS	LET
λ (Å)	6.47	6.61	6.64	—
μ (deg)	1.5	1.5	0.8	—
θ	75.5°	82.5°	87.5°	—
$cot\ \theta$	0.26	0.13	0.04	—
$d\Omega$	0.6	0.6	0.2	3.1
Φ	1.0×10^8	2.9×10^7	1.0×10^7	—
Gain	330	49	1	2.5
ΔE (μev)	11.3	5	17.5	21

This effect can clearly be seen in Fig. 2b which shows the McStas simulations; each curve represents the time-of-flight spectrum for a different pixel. Each of these spectra is then analysed separately in the software with its own final energy before being converted to energy transfer, shown in Fig. 3. The FARO approach effectively removes the effect of the large mosaic spread on the energy resolution, as the resolution is dominated now by the angular uncertainties of the sample and pixel sizes, which were 1 cm and 0.5 cm in the simulation. This encoding of the final energy with pixel position allows us to achieve good energy resolution without the usual sacrifice of count rate. Unlike the traditional inverted geometry instrument design, the resolution is however now rather sensitive to the sample geometry. In our example, with 1 cm sample height the simulations show an energy resolution of 11.7 μeV full-width half-maximum (FWHM) (see Table 1, column SHERPA TS1).

The initial simulations considered that SHERPA would replace Iris and would thus be situated on the current beam port viewing the hydrogen moderator on TS1. A possible alternative position is offered by a currently unoccupied beam port on the west side of Target Station 2 (TS2), between the future εMAP and existing IMAT instruments. In this position. SHERPA would take advantage of a much sharper neutron pulse from the solid methane moderator on TS2. This improved resolution and dynamic range, due to the lower repetition rate of TS2, comes at a price, with a reduction in count rate for the TS2 versus the TS1 instrument. Also, to match the improved resolution of the primary spectrometer, the secondary spectrometer needs to be moved further from the sample, from approximately 1 m to 1.3 m, to reduce the sample-size effect on the resolution thus also adding to the cost.

In Fig. 3 we show the resolutions for the TS1 and TS2 options based on our simulations (here we assume that guide transmission is the same for both options). A slight improvement of the line shape of SHERPA on

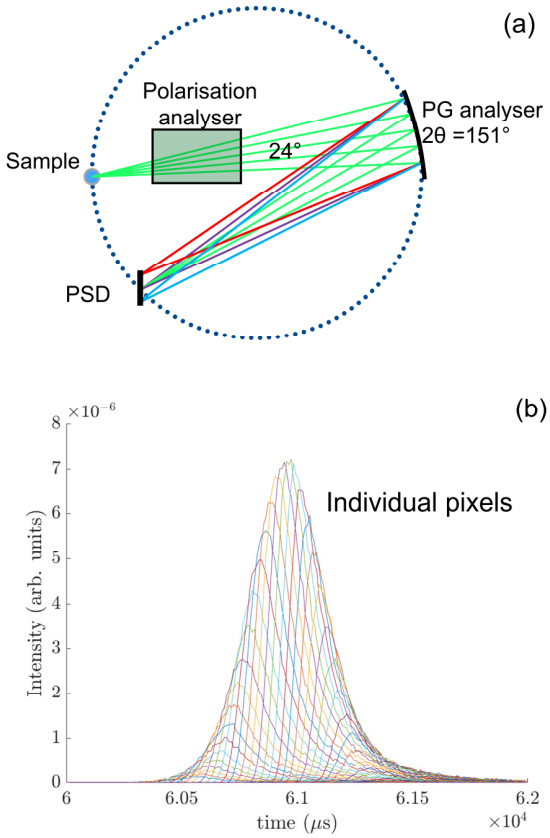

Fig. 2. (a) Prismatic effect on the energy analyser of SHERPA. The rectangular between sample and energy analyser shows schematically the position of the polarisation analyser (discussed in the next section) (b) Spectra for individual pixels.

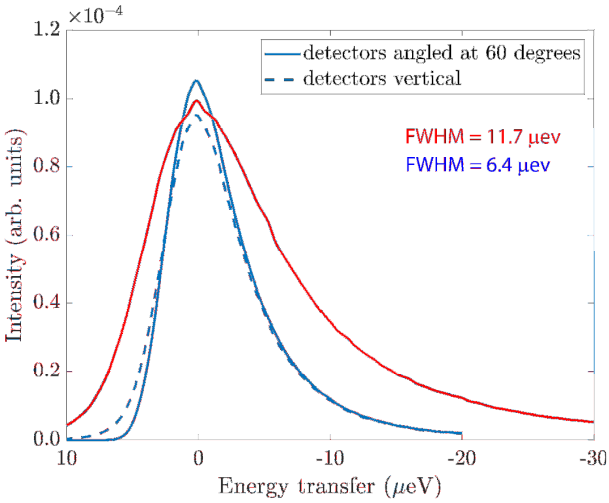

Fig. 3. McStas simulation of SHERPA energy resolution for TS1 and TS2 options, both with a sample at 35 m. The solid red line indicates SHERPA on TS1. The solid blue line is SHERPA on TS2 with detectors tilted 60° towards the Rowland circle, and the dashed blue line is with the detectors vertical.

TS2 can be achieved by tilting the detectors close to the Rowland circle at 60 degrees. The simulated detector intensity in the figure also gives an indication of the relative performance for the same conditions, namely 1 μA proton current on the target. The integral under the TS2 curve is 1.7 smaller and since the current to TS2 is 4 times smaller than to TS1, it means that the SHERPA

count rate on TS2 would be approximately 7 times smaller than if installed on TS1.

5 Polarisation analysis at SHERPA

5.1 Polariser

SHERPA is intended to support a uniaxial polarisation analysis mode. Due to its operational simplicity, we have chosen a supermirror polariser, to be installed on a guide changer. The setup is similar to the one used on the LET instrument at ISIS,[26] but an adiabatic fast-passage radio-frequency flipper will be used instead of a precession coil flipper due to its higher performance at long wavelengths and the absence of material in the beam. When SHERPA is use in unpolarised mode, the polarizer will be replaced by a section of regular neutron guide (see Fig. 1.). The cross-section of the polarising section should be exactly the same as a regular one.

We have performed some preliminary optimization of the design using McStas simulations. Results suggest a 1 m long polarising section consisting of 4 channels with absorbing walls in between. Each channel contains a polarising V-cavity, where the polarising supermirrors are coated on both sides with m = 5.5 Fe/Si supermirror. The coating of the outer walls of the device will have $m = 4$, like the non-polarising guide it replaces. The device will be placed in the section of the guide where the divergence is lowest, so as to maximise the wavelength range.

With this set-up, the expected transmission and polarisation for the SHERPA polariser are shown in Fig. 4. In the wavelength range of interest (~6.5 Å, see Table 1) the combined polariser-guide system yields good values for both transmission (~30%) and polarisation (> 95% above the cut-off wavelength).

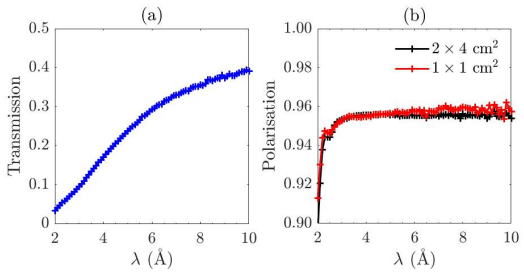

Fig. 4. Transmission of SHERPA polariser and polarisation at the sample position as a function of neutron wavelength. Polarisation is calculated for two characteristic typical sizes: 1×1 cm² and 2×4 cm² (width × height). The similarity between the curves indicates good homogeneity of the polarisation.

5.2 Analyser

The choice of polarisation analyser is less straightforward: since the final neutron energy will be relatively low (E_f ~ 1.9 meV), both supermirror and ^{3}He-based devices are possible. The latter would either correspond to a replaceable wide-angle cell close to the sample position, as implemented on LET,[7] or an in-situ pumped cell between the analyser and detectors. While the replaceable cell would imply a time-dependent beam polarization and transmission, the in-situ option suffers from the spatial constraints of the secondary spectrometer and limitations on the maximum height of the cell. Regarding supermirror devices, both a multi-channel single-bounce reflection device and multi-channel transmission device are viable.

The former would have the advantage of suppressing unwanted $\lambda/2$ neutrons, although it would require at least one side of the instrument to be permanently polarized and would need to be placed at a large distance from the sample to improve transmission. Besides, with reflection device it is much more challenging to preserve the neutron phase space, whereas for transmission one it is provided naturally. Given these disadvantages, and the inherent operational difficulties of using ^{3}He, a wide-angle transmission-based supermirror device is the current preferred options. This will have similarities with the design presented in [27], although the collimator will be integrated in the analyzer and the channels changed from Z- to V-cavities to suppress spurious multiple reflections (see Fig. 5).

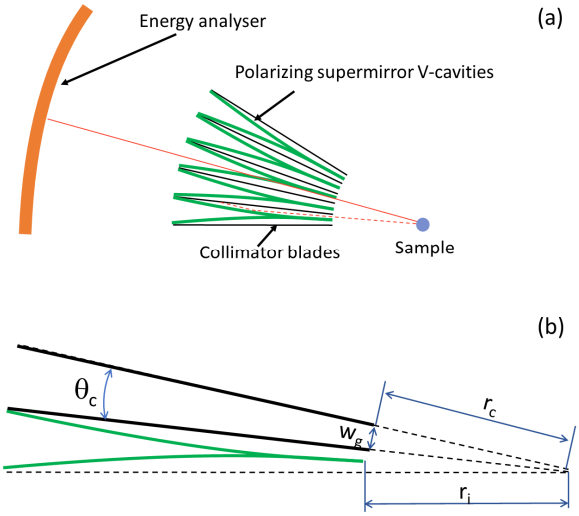

Fig. 5. (a)Schematic layout of the polarisation analyser. Polarizing cavities are shown in green. Black lines in between are collimator blades made from absorbing material. The solid red line indicates the transmitted neutron path from sample to energy analyser. The dashed one shows the path of a neutron with opposite polarization which has been absorbed. (b) Definitions of the analyser geomtertical parameters used in the text and in the next figure: angular opening of the channel θ_c, inner radius of the supermirror assembly r_i, inner radius of the collimator blade r_c. To keep enough space for the notation, in the upper channel we show only collimator blades without the supermirror cavity. Note: r_i and r_c are two different parameters. They not necessarily equal one to another, and in the optimisation calculations are varied independently.

To illustrate the performance of the device, in Fig. 6 (a-c) we plot the dependence of minimum transmitted wavelength from geometrical parameter and sample diameter. Fig.6d shows the relation between channel parameters.

The minimum inner radius is limited by dimensions of standard sample environment to be used (e.g. cryostat). The outer radius is fixed to 0.5 m, which would permit it to be accommodated in the sample area. A possible compromise between polarisation, transmission, and cost is found for a sample diameter of 12.5 mm, inner radius of 0.35 m, and angular opening of 1.3 degrees. The analyser parameters will be fully optimised once a final decision on the analyser type is made. However, it is evident that it will be possible to analyse neutrons at this wavelength even for large sample diameters and compact device dimensions, leaving sufficient space around the sample for sample environment. Irrespective of the final choice of analyser, it is expected that very good performance ($a > 0.95$, for a 1cm diameter sample, where for analyser efficiency we use the definition of [28]) can be achieved.

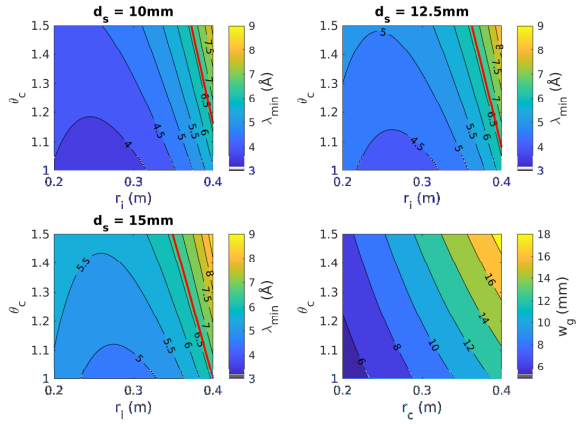

Fig. 6. (a-c) Minimum transmitted neutron wavelength versus the angular opening of the channels (θ_c, see Fig. 5b) and the inner radius of supermirror assembly without radial collimators (r_i) for sample diameter of 10 mm (a), 12.5 mm (b), and 15 mm (c). The final wavelength of the PG (002) analyser is indicated by a solid red line. (d) The gauge width accepted by the device as a function of the angular opening of the channel and the inner radius of the collimating blades.

6 Discussion and concluding remarks

Based on the above-presented simulations, we can summarize that both TS1 and TS2 option provide considerable gain in count rate compared to Iris (see Table 1). Although the gain of 330 at TS1 is particularly impressive, the factor of 49 at TS2 is already enough to get access to the experiments with weaker scattering/smaller samples as requested by the user community. On the other side, energy resolution for TS1 option is just slightly better than the one we have at Iris, while at TS2, SHERPA may have ~2.5 better energy resolution. Besides, positioning SHERPA at TS2 allows to extend the available dynamic range up to 5 meV (instead of 1 meV at current Iris, and the TS1 SHERPA option). All together, these will extend the capabilities of the instrument for the core users of Iris with biological, soft matter and functional materials. Therefore, for the moment we consider building SHERPA at TS2 as the more favourable option.

It is also important to note that completely new functionality is coming with implementation of backscattering PA-QENS. Its increased flux at low energy transfer is of interest to many other research fields. The combination of *routine* PA with ~5-10 μeV-scale resolution makes SHERPA unique and promises to revolutionise the QENS technique.

This work was supported by the Science and Technology Facilities. The authors thank A. Arbe, H. Bordallo, M. Karlsson, A. O'Malley, M. Månsson and M. Nagao for sharing their vision of requirements for polarized QENS instrument, and all participants of the SHERPA workshop and the QENS/WINS conference for fruitful discussion and giving their feedback.

References

1. W.P. Gates, T. Seydel, H. N. Bordallo, Appl. Clay Sci. **201**, 105928 (2021)
2. A. J. O'Malley, M. Sarwar, J. Armstrong, C. R. A. Catlow, I. P. Silverwood. A. P. E. York, I. Hitchcock, Phys. Chem. Chem. Phys. **20**, 11976 (2018)
3. A. Faraone, C. Branca, S. Magazu, G. Maisano, H. D. Middendorf, P. Migliardo, V. Villari, Physica B Condens. Matter **276**, 524 (2000)
4. A. Arbe, F. Alvarez, J. Colmenero, Polymers (Basel) **12**, 3067 (2020)
5. R. J. S. Lima, D. V. Okhrimenko, S. Rudić, M. T. F. Telling, V. García Sakai, D. Hwang, G. Barin, J. Eckert, J-W. Lee, H. N. Bordallo, ACS Appl. Mater. Interfaces **12**, 58161 (2020)
6. F. Nemoto, M. Kofu, M. Nagao, K. Ohishi, S. Takata, J. Suzuki, T. Yamada, K. Shibata, T. Ueki, Y. Kitazawa, M. Watanabe, O. Yamamuro, J. Chem. Phys. **149**, 054502 (2018)
7. T. Burankova, J. F. Mora Cardozo, D. Rauber A. Wildes, J. P. Embs, Sci.Rep. **8**, 16400 (2018)
8. M. Coduri, M. Karlsson, L. Malavasi J. Mater. Chem. A, **10**, 5082 (2022)
9. F. Juranyi, M. Månsson, J. L. Gavilano, M. Mena, E. Pomjakushina, M. Medarde, J. Sugiyama, K. Kamazawa, B. Batlogg, H. R. Ott, T. Seydel, EPJ Web of Conferences **83**, 02008 (2015)
10. A. Arbe, G. J. Nilsen, J. R. Stewart, F. Alvarez, V. García Sakai, J. Colmenero, Phys. Rev. Res. **2**, 022015(R) (2020)
11. G. Cassella, J. R. Stewart, G. M. Paternò, V. García-Sakai, M. Devonport, P. J. Galsworthy, R. I. Bewley, D. J. Voneshen, D. Raspino, G. J. Nilsen, J. Phys. Conf. Ser. **1316**, 012007 (2019)
12. T. Burankova, R. Hempelmann, A. Wildes, J. P. Embs, J. Phys. Chem. B **118**, 14452 (2014)
13. W. Chen, S. Watson, Y. Qiu, J. A. Rodriguez-Rivera, A. Faraone, Phys. B: Condens. Matter **564**, 166 (2019)
14. https://www.isis.stfc.ac.uk/Pages/iris.aspx (accessed 20 October 2022)

15. https://www.isis.stfc.ac.uk/Pages/osiris.aspx (accessed 20 October 2022)
16. M. Telling, private communication
17. A. Perrichon, F. Demmel, Nuclear Inst. and Methods in Physics Research, A 1039, 167014 (2022)
18. A. Perrichon, F. Fernandez-Alonso, M. Wolff, M. Karlsson, F. Demmel, J. Surf. Invest. X-ray, Synchrotron Neutron Tech., **14**, S169 (2020)
19. A. Perrichon, F. Fernandez-Alonso, M. Wolff, M. Karlsson, F. Demmel, Nuclear Inst. and Methods in Physics Research, A **947**, 162740 (2019)
20. C. J. Carlile, M. A. Adams, Physica B **182**, 431 (1992)
21. K. Lefmann, K. Nielsen, Neutron News **10**, 20 (1999)
22. P. Willendrup, E. Fahri, K. Lefmann, Physica B **350**, E735 (2004)
23. P. Willendrup, K. Lefmann, J. Neutron Res. **23**, 7 (2021)
24. R. Bewley, Rev. Sci. Instrum. **90**, 075106 (2019)
25. R. Bewley, Nuclear Inst. and Methods in Physics Research, A **998**, 165077 (2021)
26. J. Košata, G.J. Nilsen, M. Devonport, R.I. Bewley, D.J. Voneshen, P.J. Galsworthy, D. Raspino, J.R. Stewart, Physica B: Condensed Matter **551**, 476 (2017)
27. P. Böni, C. Schanzer, M. Schneider, Nuclear Inst. and Methods in Physics Research, A **966**, 163858 (2020)
28. A. R. Wildes, Neutron News, **17**, 17 (2006)